Title

CALCULATED REFLECTIVITY, MODULATED REFLECTIVITY AND BAND STRUCTURE OF GaAs, GaP, ZnSe AND ZnS

Authors

Walter, John P.
Cohen, Marvin L.

Publication Date

1969-02-01

Submitted to Physical Review

UCRL-18783
Preprint

CALCULATED REFLECTIVITY, MODULATED REFLECTIVITY AND BAND STRUCTURE OF GaAs, GaP, ZnSe AND ZnS

John P. Walter and Marvin L. Cohen

February 1969

AEC Contract No. W-7405-eng-48

LAWRENCE RADIATION LABORATORY
UNIVERSITY of CALIFORNIA BERKELEY

UCRL-18783

DISCLAIMER

UCRL-18783

Calculated Reflectivity, Modulated Reflectivity and Band Structure of GaAs, GaP, ZnSe and ZnS.*

John P. Walter† and Marvin L. Cohen

Inorganic Materials Research Division, Lawrence Radiation Laboratory,
Department of Physics, University of California,
Berkeley, California

ABSTRACT

We have calculated the electronic energy band structure, the imaginary part of the frequency dependent dielectric function, the reflectivity, and the modulated reflectivity (derivative of the reflectivity) for GaAs, GaP, ZnSe, and ZnS using the Empirical Pseudopotential Method. A direct comparison of the measured and calculated reflectivities are made. The calculated derivative of the reflectivity spectrum is compared with thermo-reflectance data.

* Supported in part by the National Science Foundation.

† NSF Graduate Fellow.

Introduction

We have calculated the electronic energy band structure, the imaginary part of the frequency dependent dielectric function, $\epsilon_2(\omega)$, the reflectivity, $R(\omega)$, and the modulated reflectivity (derivative of the reflectivity), $\Delta R/R$, for GaAs, GaP, ZnSe and ZnS using the Empirical Pseudopotential Method [1] (EPM). In previous calculations [2] the imaginary part of the frequency dependent dielectric function, $\epsilon_2(\omega)$, was calculated and compared with experiment. However, since, the reflectivity is the actual quantity measured, it was felt that a direct comparison between measured and theoretically calculated reflectivity would be desirable. The main reason for wanting a comparison of this type rather than an $\epsilon_2(\omega)$ comparison is that it is necessary to use an integral transform of the reflectivity over a large energy range to obtain $\epsilon_2(\omega)$ and the experimental reflectivity is usually known only over a limited range of energy.

In the theoretical calculation, $\epsilon_2(\omega)$ is obtained and a Kramers - Kronig analysis is still necessary; however, there are several reasons for believing that the problems in this case are less severe. First the experimental spectrum may contain exciton effects and this may cause some structure to be weighted in a manner such that a subsequent comparison of theory and experiment is difficult. Second, it is usually possible to calculate the theoretical $\epsilon_2(\omega)$ over a larger energy range than the experimental measurements and to use tail functions to accurately represent the contributions from the higher bands. Finally, surface effects can alter the heights of reflectivity peaks which, in turn, will cause energy shifts in the $\epsilon_2(\omega)$ structure. No such effects are possible in the theory calculations.

Pseudopotential form factors for these crystals were obtained by Cohen

and Bergstresser[1] (CB) using the EPM. These form factors were obtained by comparison with the existing optical data [1,3-6]. New measurements of the optical properties have been made [7-13] since that time. The results of these measurements and a direct comparison between the experimental and the theoretical $R(\omega)$ were used to make slight adjustments of the CB form factors.

We have made a critical point analysis to identify the optical structure in terms of interband transitions. The symmetries and positions in energy of the important critical points have been determined and their contributions to $\epsilon_2(\omega)$ and $R(\omega)$ have been investigated.

A comparison between theory and experiment shows good agreement for both the reflectivity and the modulated reflectivity. The latter is compared only with thermoreflectance data[7] and not with other modulated reflectance data, e.g. electroreflectance. The reason for this restriction to thermo-reflectance is that other methods, such as electroreflectance, involve a more complicated variation of the reflectivity and consequently a simple derivative of the type we have calculated is not appropriate for comparison.

Calculations

The EPM involves adjusting pseudopotential form factors to achieve good agreement with experimental results for the principal optical transitions. These form factors are then used to determine the electronic energy bands on a fine mesh of points in the Brillouin zone.

The pseudopotential Hamiltonian has the form

$$H = -\frac{\hbar^2}{2m}\nabla^2 + V(\underset{\sim}{r}) \,. \qquad (1)$$

The weak pseudopotential $V(\underset{\sim}{r})$ is expanded in the reciprocal lattice

$$V(\underset{\sim}{r}) = \sum_{|\underset{\sim}{G}|} V(\underset{\sim}{G})\, e^{-1\, \underset{\sim}{G} \cdot \underset{\sim}{r}}, \qquad (2)$$

where $\underset{\sim}{G}$ is a reciprocal lattice vector. $V(\underset{\sim}{G})$ can be conveniently expressed as

$$V(\underset{\sim}{G}) = V^S(\underset{\sim}{G}) \cos \underset{\sim}{G} \cdot \underset{\sim}{\tau} + i\, V^A(G) \sin \underset{\sim}{G} \cdot \underset{\sim}{\tau} \qquad (3)$$

where $\underset{\sim}{\tau} = a/8\,(111)$ and a is the lattice constant. In these calculations only the six form factors $V^S(111)$, $V^S(220)$, $V^S(311)$, $V^A(111)$, $V^A(200)$, and $V^A(311)$ are allowed to be non-zero; i.e., zero values are taken for $G^2 \geq 12$ and when the structure factors, $\cos \underset{\sim}{G} \cdot \underset{\sim}{\tau}$ and $\sin \underset{\sim}{G} \cdot \underset{\sim}{\tau}$, are zero.

The solution of (1), using the form factors in (3), allows a calculation of $E(\underset{\sim}{k})$ at many points in the Brillouin zone. This permits us to calculate the imaginary part of the dielectric function using

$$\epsilon_2(\omega) = \frac{e^2\hbar^2}{3\pi m^2\omega^2} \sum_{c,v} \int \delta(E_c(\underset{\sim}{k}) - E_u(\underset{\sim}{k}) - \hbar\omega)\, |< U_{\underset{\sim}{k},v} | \nabla | U_{\underset{\sim}{k},c} >|^2\, d^3k, \qquad (4)$$

where $U_{\underset{\sim}{k},v}$ and $U_{\underset{\sim}{k},c}$ are the periodic parts of the valence and conduction band wave functions and the integration is performed over the entire Brillouin zone. The summation is over the highest three valence bands and the lowest six conduction bands. $\epsilon_2(\omega)$ is calculated precisely as described by Saslow, et. al., [2] with the one modification that each cube is divided into 512 equal subcubes.

An analytic tail replaces the calculated $\epsilon_2(\omega)$ for higher energies. This is done to account for the high energy transitions which are not represented in our nine band $\epsilon_2(\omega)$ calculation. The tail function used is $\dfrac{\beta\omega}{(\omega^2 + \gamma^2)^2}$,

where $\gamma = 4.5$ eV and β is determined by continuity with $\epsilon_2(\omega)$ at the energy where the transitions neglected in our band cut-off become important. The tail function begins at 8.85 eV for GaAs, 8.95 for GaP, 10.85 for ZnSe, and 10.95 for ZnS. A Kramers-Kronig transformation gives $\epsilon_1(\omega)$; this function together with $\epsilon_2(\omega)$ allows a calculation of the reflectivity $R(\omega)$.

The Cohen and Bergstresser pseudopotential form factors were used as our starting point. By the process described above, we calculated $\epsilon_2(\omega)$ and $R(\omega)$ and then compared $R(\omega)$ with the experimental reflectivity. Much of the gross detail was the same and thus the most important identifications were easily made. By varying the form factors slightly we attempted to move the major peaks to agree more closely to experiment and to duplicate the finer structure. The CB form factors were constrained in the following way: the symmetric form factors for GaAs and ZnSe were made to agree with the Ge potential, which is in the same row of the Periodic Table; the GaP and ZnS symmetric form factors were set equal to an average of the Group IV elements corresponding to the rows involved, i.e., an average of Si and Ge. This constraint was relaxed when we made our "fine" adjustment of the form factors. A comparison of the CB form factors and those used in the present calculation are given in Table I. The largest variation is about 0.02 Rydberg.

In order to shift the reflectivity peaks or shoulders in a predictable manner, we had to determine the transitions responsible for the major contributions to these structures. This was done by finding the energy of the desired peak or shoulder on the $\epsilon_2(\omega)$ graph and then examining the contributions to ϵ_2 at that energy from the constituent interband transitions.

When we had determined the interband transition contributing the greatest amount, e.g., band 4 to band 5, we examined a table of energy differences for these bands throughout the Brillouin zone. Particular attention was given to locating critical points with energy in the vicinity of the energy of the optical structure, although volume effects and the relative size of the momentum matrix elements were also used to determine the probable origin of the structure; the ultimate test of the correctness of our labelling was to change the pseudopotential slightly, to note how the energy splitting changed at that transition point, and finally to see if the peak position changed by the same amount as the energy splitting. All of the prominent reflectivity structure was labelled by this procedure.

To further elucidate this procedure, let us examine the large ϵ_2 peak which occurs at 4.7 eV for GaAs. The value of ϵ_2 at that energy is 31.0. From our tables of interband transitions the major contributions to that peak are bands (4-5), 26.2, bands (3-5), 2.7, bands (4-6), 1.4, with other bands contributing even smaller amounts. Thus transitions from bands (4-5) are almost totally responsible for this peak. An examination of the energy differences between bands 4 and 5 throughout the Brillouin zone reveals that an M_2 critical point occurs along the Σ direction at 4.76 eV with large oscillator strength. Furthermore, we observe that if by varying the form factor slightly the energy splitting at that point is changed by an amount Δ, then the position of the ϵ_2 peak changes by Δ with insignificant error. We therefore conclude that the GaAs peak at 4.7 eV can be labelled by the transition $\Sigma_2 - \Sigma_1$.

For the determination of the form factors from the experimental data, six structural features of R (ω) are chosen as being particularly descriptive

of that function. These structures include the basic gap and the major peaks. In order to determine how the form factors should be varied, we use the following expression:

$$E_i = E_i^{\circ} - \sum_{j=1}^{6} \left(\frac{\partial E_i}{\partial F_j}\right)^{\circ} \left(F_j - F_j^{\circ}\right), \qquad (5)$$

where the F_j° are the six non-zero CB form factors and the E_i° are the six characteristic energy splittings. $\left(\frac{\partial E_i}{\partial F_j}\right)^{\circ}$ are the derivatives of the characteristic energy splittings with respect to the form factors, evaluated at the CB form factors. The E_i are the experimental characteristic splittings and the F_j are the new form factors. In practice this equation is useful only in the range $|F_j - F_j^{\circ}| \leq .01$ Ry. If we define $\Delta E_i \equiv E_i - E_i^{\circ}$, $\Delta F_j \equiv F_j - F_j^{\circ}$, and $A_{ij} \equiv \left(\frac{\partial E_i}{\partial F_j}\right)^{\circ}$, equation (5) may be written

$$\Delta E_i = \sum_{j=1}^{6} A_{ij}\, \Delta F_j, \text{only if } |\Delta F_j| \leq .01 \ . \qquad (6)$$

The terms ΔE_i are known and the terms A_{ij} can be easily calculated. This equation cannot be merely inverted because the ΔE_i are sufficiently large for some j that $|\Delta F_j| > .01$, and consequently the equation (6) no longer correctly describes the situation. We therefore use a gradient projection method of nonlinear programming.[14] The function

$$P = \sum_{i=1}^{6} \left(\Delta E_i - \sum_{j=1}^{6} A_{ij}\, \Delta F_j\right)^2$$

is a measure of the goodness of the fit to the experimental points. P is minimized subject to the constraints $|\Delta F_j| \leq .01$. P must decrease if the matrix

Λ is non-zero, but if P is still too large after this process is completed, the new form factors replace the old and the process is repeated. We have found it necessary to perform at least two iterations before satisfactory agreement is achieved between theory and experiment at the characteristic points. This procedure does not guarantee that P can be made equal to zero but after each iteration P can be no larger than the previous P. We note, however, that the final form factors do not necessarily constitute a unique solution to the problem.

For GaAs, the following six splittings and identifications are used to characterize R (ω): $\Gamma_{15} - \Gamma_1$ (1.48 eV), $L_3 - L_1$ (2.68 eV), $\Sigma_2 - \Sigma_1$ (4.75eV), $\Delta_5 - \Delta_1$ (4 - 6) (5.55eV), volume effect (4 - 6) (6.35eV), and $L_3 - L_3$ (6.40eV). For GaP, $\Gamma_{15} - \Gamma_1$ (2.80eV), $L_3 - L_1$ (3.45eV), $\Sigma_2 - \Sigma_1$ (5.12eV), volume effect (4 - 6) (6.52eV), $L_3 - L_3$ (6.60eV), and $\Lambda_3 - \Lambda_3$ (6.60eV). For ZnSe, $\Gamma_{15} - \Gamma_1$ (2.90eV), $L_3 - L_1$ (4.75eV), $\Sigma_2 - \Sigma_1$ (6.75eV), $\Delta_5 - \Delta_1$ (4 - 6) (7.00eV), volume effect (4 - 6) (8.25eV), and $\Lambda_3 - \Lambda_3$ (8.75eV). For ZnS, $\Gamma_{15} - \Gamma_1$ (3.72eV), $L_3 - L_1$ (5.55eV), $\Sigma_2 - \Sigma_1$ (7.00eV), $\Delta_5 - \Delta_1$ (4 - 6) (7.35eV), volume effect (4 - 6) (8.35eV), and $\Lambda_3 - \Lambda_3$ (8.75eV).

Results

The band structures in the principal symmetry directions and graphs of selected optical functions are shown in Figures 1 - 15. Table I presents a comparison of the CB form factors and those derived in this work. Tables II - V tabulate the important critical points for the four compounds.

GaAs. (Figures 1 - 4)

The threshold in $\epsilon_2(\omega)$ at 1.46eV is caused by $\Gamma_{15} - \Gamma_1$ transitions. The rise and peak in the 2.7 - 3.1eV region corresponds to $L_3 - L_1$ transitions at 2.69eV and $\Lambda_3 - \Lambda_1$ transitions at 2.93eV. The prominent peak at 4.7eV is

caused almost enitrely by $\Sigma_2 - \Sigma_1$ transitions in the vicinity of (.58,.58,0) (units of $2\pi/a$). Some contribution comes from the shoulder on the left side of the peak; this shoulder is attributed to transitions $\Delta_5 - \Delta_1$ (M_0 singularity) at 4.10 eV, $\Delta_5 - \Delta_1$ (M_1) at 4.23eV, and $X_5 - X_1$ (M_1) at 4.34eV. The (4 - 6) transitions are insignificant in their contribution relative to (4 - 5) transitions in the vicinity of this peak. The $X_5 - X_3$ transitions at 4.59eV and $\Gamma_{15} - \Gamma_{15}$ transitions at 4.82eV create no discernible structure. Changing the energy splittings for these transitions causes no noticeable change in the peak structure. The small peak at 5.7eV is attributed to $\Delta_5 - \Delta_1$ (4 - 6) transitions at 5.69eV. The last major peak at 6.35eV is caused almost entirely by (4 - 6) transitions within the Brillouin zone in the vicinity (.57, .43, .29). Some contribution does come from $L_3 - L_3$ transitions at 6.45eV, but most of the contribution is from the volume effect. The shoulder at 6.5eV is caused by $\Lambda_3 - \Lambda_3$ transitions, and the last shoulder arises from a volume effect caused by (4 - 7) transitions.

Plots of both theoretical and experimental reflectivity appear in Figure 3. The first peak after the small structure at threshold corresponds to the Λ peak occuring at 3.1eV in $\epsilon_2(\omega)$. The shoulder on the main peak in the reflectivity corresponds to the shoulder on the main ϵ_2 peak and in general each piece of structure in the reflectivity plot has its counterpart on the ϵ_2 plot, displaced by at most 0.25eV. The experimental reflectivity shows a doublet peak at 2.90eV and 3.14eV which is attributed to spin-orbit splitting. In addition, this peak has greater magnitude than the theoretical peak. This can be attributed to exciton effects [15,16,17] which can occur at this band edge for all four compounds under consideration. Our theory does not take into account either spin-orbit splitting or exciton effects. The agreement between theory and

experiment in the vicinity of the main peak is excellent. A shoulder appears in both the experimental and theoretical reflectivity at 4.4eV. Another shoulder in the theoretical reflectivity appears at 5.65eV. This can be seen in the data of Greenaway[3] at 5.55eV and Vishnubhatla and Woolley [12] at 5.45eV. It is not present in the reflectivity of Ehrenreich and Phillip.[4] Beyond 6.0eV the experimental reflectivity no longer shows the detailed structure which appears in the theoretical reflectivity.

The $\Delta R/R\ (\omega)$ spectrum is obtained from thermoreflectance measurements by Matategui, et. al.,[11] is compared with that obtained directly from a derivative of the theoretical reflectivity. (See Fig. 4.) Since the spectrum represents the derivative of the reflectivity, it magnifies every kink in the reflectivity. Despite this, the agreement between experiment and theory for this spectrum is quite good.

GaP (Figures 5 - 8)

The threshold in $\epsilon_2(\omega)$ at 2.79eV is caused by $\Gamma_{15} - \Gamma_1$ transitions. The rise and peak in the 3.4 - 4.0eV region corresponds to $L_3 - L_1$ transitions at 3.40eV and $\Lambda_3 - \Lambda_1$ transitions at 3.76eV. The prominent peak at 5.1eV is caused almost entirely by $\Sigma_2 - \Sigma_1$ transitions in the vicinity of (.50,.50,0.). Some contribution comes from the shoulder on the left side of the peak. This shoulder is attributed to transitions $X_5 - X_1$ at 4.57eV, $\Delta_5 - \Delta_1\ (M_0)$ at 4.50eV, and $\Delta_5 - \Delta_1\ (M_1)$ at 4.72eV. Just as for GaAs, the (4 - 6) transitions are negligible compared to the (4 - 5) transitions in the vicinity of this peak. $X_5 - X_3$ transitions at 4.96eV and $\Gamma_{15} - \Gamma_{15}$ transitions at 5.23eV create no discernible structure. The peak at 6.5eV is caused by (4 - 6) transitions in a volume with center at (.50, .43, .29). The $L_3 - L_3$ transitions at 6.57eV also contribute to this peak; however, varying the

energy splitting in the vicinity of (.50,.43,.29) has considerably greater influence in changing the position of the peak than does a change in the $L_3 - L_3$ energy splitting. The small peak at 6.7eV is attributed to $\Lambda_3 - \Lambda_1$ transitions. The shoulder at 7.3eV is a volume effect caused by (4 - 7) transitions.

The experimental reflectivity shows an exciton-enhanced peak at 3.7eV, in good agreement with the theoretical peak at 3.7eV. The experimental data exhibits a shoulder at 4.6eV, which corresponds to the theoretical result of 4.7eV. The major peak occurs at the same energy for both experiment and theory, but the peak heights disagree somewhat. The experimental peak at 6.9eV corresponds to the theoretical peaks at 6.6 and 6.9eV. The shoulder in the experimental data at 7.4eV corresponds to the theoretical peak at 7.5eV. The overall agreement between the experimental and theoretical reflectivity, especially with regard to peak positioning, is good.

A comparison of $\Delta R/R$ (ω) and the thermoreflectance measurements appears in Figure 8.

ZnSe (Figures 9 - 12)

The threshold in ϵ_2 (ω) is caused by $\Gamma_{15} - \Gamma_1$ transitions at 2.90eV. The rise and peak in the 4.5 - 4.9eV region corresponds to $L_3 - L_1$ transitions at 4.59eV and $\Lambda_3 - \Lambda_1$ transitions at 4.73eV. The prominent peak at 6.45eV is caused by $\Delta_5 - \Delta_1$ (M_1) transitions in the vicinity of (.64,0.,0.) at 6.20eV and $\Sigma_2 - \Sigma_1$ (M_2) transitions in the vicinity of (.64,.64.0.) at 6.63eV. $X_5 - X_1$ transitions at 5.99eV contribute only slightly to the peak. The small peak at 7.2eV is caused by (4-6) transitions in the Δ direction at 7.06eV (M_o) and 7.23eV (M_1). The shoulder at 7.55eV is attributed to (3-6) (M_1) transitions along Σ at 7.48eV.

$\Gamma_{15} - \Gamma_{15}$ transitions occur at 7.84eV. The peak at 8.25eV is caused by (4-6) transitions in a volume centered at (.64,.43,.29), which is along the KL line near L. The peak at 8.85eV is caused chiefly by (4-7) and (3-6) transitions in the Λ direction in the vicinity of (.36,.36,.36). The shoulder at 9.35eV is caused by (3-7) transitions in a volume centered at (.43,.14,.07).

The theoretical and experimental reflectivity appear in Fig. 11. The experimental peak at 4.85 corresponds to the spin-orbit split experimental peak at 4.75eV and 5.05eV. The theoretical peak is of the same magnitude as the experimental peaks, but it is displaced from the center of the two experimental peaks by .05eV. The next experimental peak occurs at 6.63eV and has the same shape and roughly the same magnitude as the theoretical peak at 6.65eV. The experimental reflectivity shows a small peak at 6.0eV which does not appear in the theoretical reflectivity. However, the $X_5 - X_1$ critical point at 5.99eV could explain it, since spin-orbit splittings would slightly flatten the bands at X. The theoretical shoulder at 7.3eV corresponds to the shoulder at 7.25eV in the experimental data. The steeper slope of the low temperature data on the right side of the main peak indicates that a low temperature study in the region of 6.9 - 7.2eV might reveal a dip similar to that appearing in the theoretical reflectivity. Another experimental shoulder appears at 7.6eV, corresponding to a slight shoulder at 7.55eV for the theoretical reflectivity.

The small peak in the experimental data at 7.8eV is attributed to $\Gamma_{15} - \Gamma_{15}$ transitions. Although this peak does not appear in the theoretical reflectivity, we expect that the spin-orbit splitting would flatten the bands near Γ and produce this small peak. Since the theoretical peak at 8.35eV is caused

by transitions near L, we expect the peak to be spin-orbit split in the experimental reflectivity. The experimental data does show two peaks at 8.28eV and 8.46eV. The next theoretical peak at 9.05eV is caused by Λ transitions; the corresponding experimental peaks are spin-orbit split at 8.97 and 9.25eV. The somewhat flat theoretical peak at 9.6eV corresponds to the experimental peak at 9.7eV.

The agreement between experiment and theory is good for ZnSe. In most cases the location of the structure in energy, the shape of the structure and the height of the structure is the same for theory and experiment.

A comparison of $\Delta R/R$ (ω) and the thermoreflectance appears in Figure 12.

ZnS (Figures 13-15)

The threshold in $\epsilon_2(\omega)$ is caused by $\Gamma_{15} - \Gamma_1$ transitions at 3.74eV. The rise and peak in the 5.4 - 5.7eV region is caused by $L_3 - L_1$ transitions at 5.40eV and $\Lambda_3 - \Lambda_1$ transitions at 5.52eV. The principal contributions to the peak at 7.0eV comes from $\Sigma_2 - \Sigma_1$ transitions at 7.08eV located near (.54,.54,0.) and from $\Delta_5 - \Delta_1$ transitions at 6.99eV located near (.50,0.,0.). The $X_5 - X_1$ transitions at 6.31eV also contribute to the peak, causing the slight bulge at 6.5eV. The small peak at 7.5eV is caused by (4-6) transitions in the Δdirection at 7.45eV and 7.57eV. The peak subsides with $\Gamma_{15} - \Gamma_{15}$ transitions at 7.79eV. The peak at 8.35eV is caused by (4-6) transitions in a volume centered at (.57,.36,.14). Although $L_3 - L_3$ transitions also occur at 8.35eV, changing the energy splitting has negligible effect on the peak, whereas changing the splitting in the vicinity of(.57,.36,.14)does change the position of the peak by an amount equal tothe change in the splitting. The peak at 8.65eV is

caused principally by (3-6) transitions in the Λ direction. The next two pieces of structure at 8.85 and 9.5 eV are attributed to (3-6) and (4-7) volume transitions.

The data of Cardona and Harbeke[6] and of Baars[9] show a small peak at 3.7eV. The theoretical counterpart is a bump at 3.8eV. The experimental data shows an exciton-enhanced peak at 5.8eV. The theoretical peak occurs at 5.6eV, giving only fair agreement with experiment. The main theoretical peak occurs at 7.05eV; the measured value is 6.99eV [6] and 7.02eV [9]. Shoulders appear in the experimental data at 7.4 and 7.9 eV for Cardona and Harbeke and at 7.5eV for Baars. The corresponding theoretical shoulder occurs at 7.55eV. Cardona and Harbeke find a 7.9eV shoulder which does not appear in the theoretical results or in Baars' data, so it must remain unexplained for the present. Baars' data exhibits peaks at 8.35, 9.0, and 9.6eV, which are in good agreement with the theoretical peaks at 8.45, 9.15, and 9.75eV. The data of Cardona and Harbeke has only one peak in this region at 9.8eV.

We consider the agreement between experiment and theory to be only "fair" compared with the agreement achieved for the other crystals. However, we should point out that there is only fair agreement between the experiments themselves. No thermo-reflectance data was available for ZnS; a theoretical curve for $\Delta R/R$ was therefore not calculated.

Discussion

We have obtained good agreement between measured and calculated reflectivity and between modulated reflectivity and thermoreflectance. The agreement appears good enough to indicate that our identifications of the important transitions are substantially correct and that our band structure is accurate in the region near the fundamental gap.

The results for GaAs and GaP are good. One point that should be discussed in detail is that in our calculations for GaAs and GaP, the shoulder on the low energy side of the main Σ peak of $\epsilon_2(\omega)$ is caused by (4-5) transitions along Δ and at X, and that the $\Gamma_{15} - \Gamma_{15}$ transitions do not contribute significantly. A careful study of our band structure reveals that it is consistent with photoemission yield data for GaAs [10,18]. As the vacuum level [18] is lowered, the first small peak is caused by (4-6) transitions at 4.60 eV along Σ at (.15,.15,0.). The photoemission yield peak becomes larger and shifts its center from 4.65 to 4.50 eV because of (4-6) transitions along Δ (with an average energy of 4.4eV) and the beginning of massive (4-5) transitions along both Δ and Σ. Eden [10] estimates that $\Gamma_{15} - \Gamma_{15}$ lies in the range of 4.6 to 4.8 eV for GaAs, in good agreement with our value of 4.8eV, and he estimates a value in the range of 4.8 to 5.2eV for GaP, as compared with our value of 5.2eV. If we allow for a small spin-orbit splitting of bands 3 and 4 along the Δ direction, our band structure is also consistent with the electroreflectance measurements of Thompson, et. al.[7]

The availability of new and precise data for ZnSe has enabled us to apply the EPM to explore the details in the reflectivity spectrum. The agreement between the calculated and measured reflectivity is very good. We believe the only real differences arise from spin-orbit contributions, and we plan to add spin-orbit terms in the near future to test this conclusion.

For ZnS the fitting procedure was difficult because the experiments differ by a fair amount. In fact, the differences between experiments is greater than that between the theory and either experiment. The agreement is only fair.

For all four crystals the calculated reflectivity at high energies has

greater magnitude than the measured reflectivity. Assuming the experimental measurements are accurate in this region, one possibility is that the pseudo-wave-functions might not give accurate oscillator strengths at higher energies. Another possibility is that the high-energy set of calculated ϵ_2 peaks (located at 6-7eV for GaAs and GaP and at 8-10eV for ZnSe and ZnS) should be smaller in magnitude and smeared over a slightly larger area, which might occur if we were to include indirect transitions and life-time effects. (The steep slope followed by the small magnitude of $\epsilon_2(\omega)$ on the high-energy side of these peaks is essentially what causes the high reflectivity.)

A comparison shows that the pseudopotentials for gallium and zinc are in reasonable agreement with the model potentials of Animalu and Heine[19]. The agreement is not precise because our pseudopotential takes into account crystalline effect and is constrained equal to zero for $G^2 < 11$.

Acknowledgements. One of us (J.P.W.) expresses his gratitude to Dr. C.Y. Fong for many helpful discussions.

This work was supported by the United States Atomic Energy Commission.

References

1. M. L. Cohen and T. K. Bergstresser, Phys. Rev. 141 , 789 (1966), and references therein.
2. W. Saslow, T. K. Bergstresser, C. Y. Fong, M. L. Cohen, and D. Brust, Solid State Comm. 5, 667 (1967).
3. D. L. Greenaway, Phys. Rev. Letters 9 , 97 (1962).
4. H. R. Philipp and H. Ehrenreich, Phys. Rev. 129, 1550 (1963).
5. M. Aven, T. F. Marple, and B. Segall, J. Appl. Phys. (Suppl.) 32, 2261 (1961).
6. M. Cardona and G. Harbeke, Physics of Semiconductors, Proc. of 7th Int. Conf. (Dunod, Paris, 1964), p. 217.
7. A. G. Thompson, M. Cardona, K.L.Shaklee, and J. C. Woolley, Phys. Rev. 146, 601 (1966).
8. F. H. Pollak, M. Cardona, and J. Barber, to be published.
9. J. W. Baars, II - VI Semiconducting Compounds, 1967 International Conference, edited by D. G. Thomas, (W.A. Benjamin, Inc., New York, 1967), p. 631.
10. R. C. Eden, Stanford Electronics Laboratory, Tech. Rep. 5222-1, 1967 (unpublished).
11. E. Matatagui, A. G. Thompson, and M. Cardona, to be published.
12. S. S. Vishnubhatla and J. C. Woolley, Can. J. Phys. 46, 1769 (1968).
13. Y. Petroff, M. Balkanski, J. P. Walter, and M. L. Cohen, to be published.
14. J. B. Rosen, J. Soc. Indust. Appl. Math. 8, 181 (1960).
15. C. Y. Fong, W. Saslow, and M. L. Cohen, Phys. Rev. 168, 992 (1968).
16. J. C. Phillips, in Solid State Physics, edited by F. Seitz and D. Turnbull (Academic Press Inc., New York, 1965), Vol. 16.

17. K. L. Shaklee, J. E. Rowe, and M. Cardona, Phys. Rev. 174, 828 (1968).

18. The experimental data of G. Gobeli and F. Allen appears in M. L. Cohen and J. C. Phillips, Phys. Rev. 139, A912(1965).

19. A.O.E. Animalu and V. Heine, Phil. Mag. 12, 1249 (1965).

Table Captions

I. A comparison of the GaAs, GaP, ZnSe, and ZnS form factors (in Ry) used in the present work (on top) with those used in Ref. 1.

II. Theoretical and experimental reflectivity structure and their identifications, including the location in the Brillouin zone, energy, and symmetry of the calculated critical points for GaAs. The experimental results are due to H. Philipp and H. Ehrenreich and appear in Ref. 10.

III. Theoretical and experimental reflectivity structure and their identifications, including the location in the Brillouin zone, energy, and symmetry of the calculated critical points for GaP. The experimental results are due to H. Philipp and H. Ehrenreich and appear in Ref. 10.

IV. Theoretical and experimental reflectivity structure and their identifications, including the location in the Brillouin zone, energy, and symmetry of the calculated critical points for ZnSe. The experimental results are due to Y. Petroff and M. Balkanski (Ref. 13).

V. Theoretical and experimental reflectivity structure and their identifications, including the location in the Brillouin zone, energy, and symmetry of the calculated critical points for ZnS. Experiment 1 refers to Aven, Marple, and Segall (Ref. 5). Experiment 2 refers to J. W. Baars (Ref. 9).

Table I

	$V^S(111)$	$V^S(220)$	$V^S(311)$	$V^A(111)$	$V^A(200)$	$V^A(311)$
GaAs	-.245	-.005	.075	.062	.035	.003
	-.23	.01	.06	.07	.05	.01
GaP	-.225	.024	.076	.128	.053	.020
	-.22	.03	.07	.12	.07	.02
ZnSe	-.223	-.008	.068	.204	.099	.022
	-.23	.01	.06	.18	.12	.03
ZnS	-.249	.038	.053	.195	.116	.015
	-.22	.03	.07	.24	.14	.04

Table II GaAs

Reflectivity Structure (eV)		Associated Critical Points		
Theory	Experiment	Location in Zone	Symmetry	CP Energy(eV)
-	1.48	$\Gamma_{15} - \Gamma_1$ (0.,0.,0.)	M_o	1.46
2.95	2.88,3.15 (spin orbit)	$L_3 - L_1$ (.5,.5,.5)	M_o	2.69
		$\Lambda_3 - \Lambda_3$ (.21,.21,.21)	M_1	2.93
4.45	4.55	$\Delta_5 - \Delta_1$ (.60,0,0.) (band 4 to band 5)	M_o	4.10
		$X_5 - X_1$ (1.,0.,0.)	M_1	4.34
4.85	5.00	$\Delta_5 - \Delta_1$ (.35, 0.,0.) (Band 4 to band 5)	M_1	4.23
		$\Sigma_2 - \Sigma_1$ (.58,.58,0.)	M_2	4.76
5.65	5.55*	$\Delta_5 - \Delta_1$ (.50,0.,0.) (band 4 to band 6)	M_1	5.69
6.45	6.6	volume effect from region around (.57,.43.,29) (band 4 to band 6)	-	6.35
		$L_3 - L_3$(.5,.5,.5)	M_2	6.45
6.75	6.6	$\Lambda_3 - \Lambda_3$(.43,.43,.43) band 3 to band 6 and band 4 to band 7	M_1	6.51
		$\Lambda_3 - \Lambda_3$ (.43,.43,.43) band 4 to band 6	M_3	6.51

*This shoulder appears in data of Greenaway (Ref. 3)

Table III GaP

Reflectivity Structure (eV)		Associated Critical Points		
Theory	Experiment	Location in Zone	Symmetry	CP Energy (eV)
-	2.80	$\Gamma_{15} - \Gamma_1$ (0.,0.,0.)	M_o	2.79
3.70	3.70	$L_3 - L_1$ (.5,.5,.5)	M_o	3.40
		$\Lambda_3 - \Lambda_1$ (.15,.15,.15)	M_1	3.76
4.7	4.6	$\Delta_5 - \Delta_1$ (.71,0.,0.) (Band 4 to band 5)	M_o	4.50
		$X_5 - X_1$ (1.,0,.0.)	M_1	4.57
5.3	5.3	$\Delta_5 - \Delta_1$ (.30,0,0.) (Band 4 to band 5)	M_3	4.72
		$\Sigma_2 - \Sigma_1$ (.50,.50,0.)	M_2	5.20
6.7	6.9	volume effect from region around (.50,.43,.29) (band 4 to band 6)	-	6.5
		$L_3 - L_3$ (.5,.5,.5)	M_2	6.57
6.9	6.9	$\Lambda_3 - \Lambda_3$ (.37,.37,.37) band 3 to band 6 and band 4 to band 7	M_1	6.68
		$\Lambda_3 - \Lambda_3$ (.37,.37,.37) band 4 to band 6	M_3	6.68

Reflectivity Structure (eV)		Table IV Associated Critical Points		
Theory	Experiment	Location in Zone	Symmetry	CP Energy (eV)
2.9	2.9	$\Gamma_{15} - \Gamma_1$ (0.,0.,0)	M_o	2.90
4.85	4.75,5.05 (spin orbit)	$L_3 - L_1$ (.5,.5,.5)	M_o	4.59
		$\Lambda_3 - \Lambda_1$ (.31,.31,.31)	M_1	4.73
–	6.00	$X_5 - X_1$ (1.,0.,0.)	M_o	5.99
6.55	6.63	$\Delta_5 - \Delta_1$ (.64,0.,0.) (Band 4 to band 5)	M_1	6.20
		$\Sigma_2 - \Sigma_1$ (.64.,64,0.) (Band 4 to band 5)	M_2	6.63
7.3	7.25	$\Delta_5 - \Delta_1$ (.41,0.,0.) (Band 4 to band 6)	M_o	7.06
		$\Delta_5 - \Delta_1$ (.57,0.,0.) (Band 4 to band 6)	M_1	7.23
7.55	7.6	$\Sigma_1 - \Sigma_1$ (.20,0.,0.) (band 3 to band 6)	M_1	7.48
–	7.8	$\Gamma_{15} - \Gamma_{15}$ (0.,0.,0.)	degenerate	7.84
8.35	8.28,8.46 (spin orbit)	volume effect from region around (.64,.43,.29) (Band 4 to band 6)	–	8.25
9.05	8.97,9.25 (spin orbit)	$\Lambda_3 - \Lambda_3$ (.36,.36,.36) (Band 4 to band 7)	M_1	8.79
		$\Lambda_3 - \Lambda_3$ (.36,.36,.36) (band 3 to band 6)	M_2	8.79
9.6	9.7	volume effect from region around (.43,.14,.07) (Band 3 to band 7)	–	9.35

Table V ZnS

Reflectivity Structure (eV)			Associated Critical Points		
Theory	Experiment 1	Experiment 2	Location in Zone	Symmetry	CP Energy(eV)
3.8	3.66,3.76 (spin orbit)	3.68,3.75 (spin orbit)	$\Gamma_{15} - \Gamma_1$ (0.,0.,0.)	M_o	3.74
5.55	5.79	5.78	$L_3 - L_1$(.5,.5,.5)	M_o	5.40
			$\Lambda_3 - \Lambda_1$ (.32,.32,.32)	M_1	5.52
6.6	-	-	$X_5 - X_1$ (1.,0.,0.)	M_o	6.31
7.05	6.99	7.02	$\Delta_5 - \Delta_1$ (.50,0.,0.) (band 4 to band 5)	M_1	6.99
			$\Sigma_2 - \Sigma_1$ (.53,.53,0.)	M_2	7.08
7.55	7.41	7.5	$\Delta_5 - \Delta_1$ (.37,0.,0.) (band 4 to band 6)	M_o	7.45
			$\Delta_5 - \Delta_1$ (.51,0.,0.) (band 4 to band 6)	M_1	7.57
-	-	-	$\Gamma_{15} - \Gamma_{15}$	degenerate	7.79
8.45	-	8.35	Volume effect from region around (.57,.36,.14) (band 4 to band 6)	-	8.35
9.15	-	9.0	$\Lambda_3 - \Lambda_3$ (.29,.29,.29) (band 3 to band 6)	M_1	8.64
			Volume effect (bands 3 to 6 and bands 4 to 7)	-	8.85
9.75	9.8	9.6	Volume effect (bands 3 to 6 and bands 4 to 7)	-	9.5

Figure Captions

1. Band structure of GaAs along the principle symmetry directions.
2. Theoretical $\epsilon_2(\omega)$ for GaAs. The tail function begins at 8.85 eV.
3. A comparison of theoretical and experimental $R(\omega)$ for GaAs. The experimental results are due to Philipp and Ehrenreich and appear in Ref. 10. The tail function begins at 8.85 for $\epsilon_2(\omega)$.
4. A comparison for GaAs of theoretical $\Delta R/R(\omega)$ with thermoreflectance measurements by Matatagui, et. al. (Ref. 11).
5. Band structure of GaP along the principle symmetry directions.
6. Theoretical $\epsilon_2(\omega)$ for GaP. The tail function begins at 8.95 eV.
7. A comparison of theoretical and experimental $R(\omega)$ for GaP. The experimental results are due to Philipp and Ehrenreich and appear in Ref. 10. The tail function begins at 8.95 eV for $\epsilon_2(\omega)$.
8. A comparison for GaP of theoretical $\Delta R/R(\omega)$ with thermoreflectance measurements by Matatagui, et. al. (Ref. 11).
9. Band structure of ZnSe along the principle symmetry directions.
10. Theoretical $\epsilon_2(\omega)$ for ZnSe. The tail function begins at 10.85eV.
11. A comparison of theoretical and experimental $R(\omega)$ for ZnSe. The experimental results are due to Y. Petroff and M. Balkanski (Ref. 13). The tail function begins at 10.85 eV for $\epsilon_2(\omega)$.
12. A comparison for ZnSe of theoretical $\Delta R/R(\omega)$ with thermoreflectance measurements by Matatagui, et. al. (Ref. 11).
13. Band structure for ZnS along the principle symmetry directions.
14. Theoretical $\epsilon_2(\omega)$ for ZnS. The tail function begins at 10.95eV.
15. A comparison of theoretical and experimental $R(\omega)$ for ZnS. Experiment 1 refers to Aven, et.al. (Ref. 5). Experiment 2 refers to J. W. Baars (Ref. 9). The tail function begins at 10.95 eV.

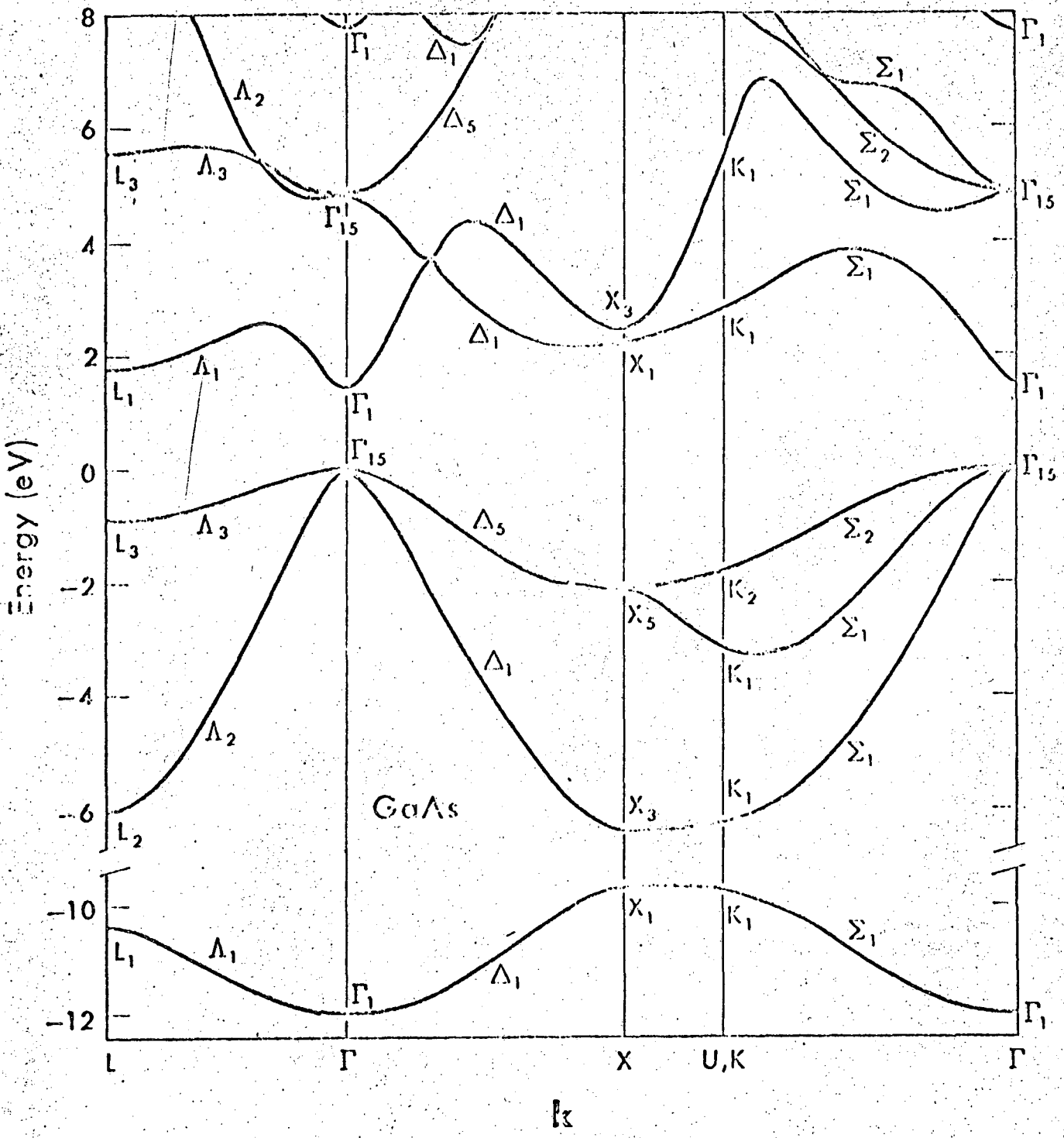
Energy (eV)
8
6
4
2
0
−2
−4
−6
−10
−12
GaAs
L
Γ
X
U,K
Γ
k
L1
L2
L3
Λ1
Λ2
Λ3
Γ1
Γ15
Δ1
Δ5
X1
X3
X5
K1
K2
Σ1
Σ2

Fig. 1

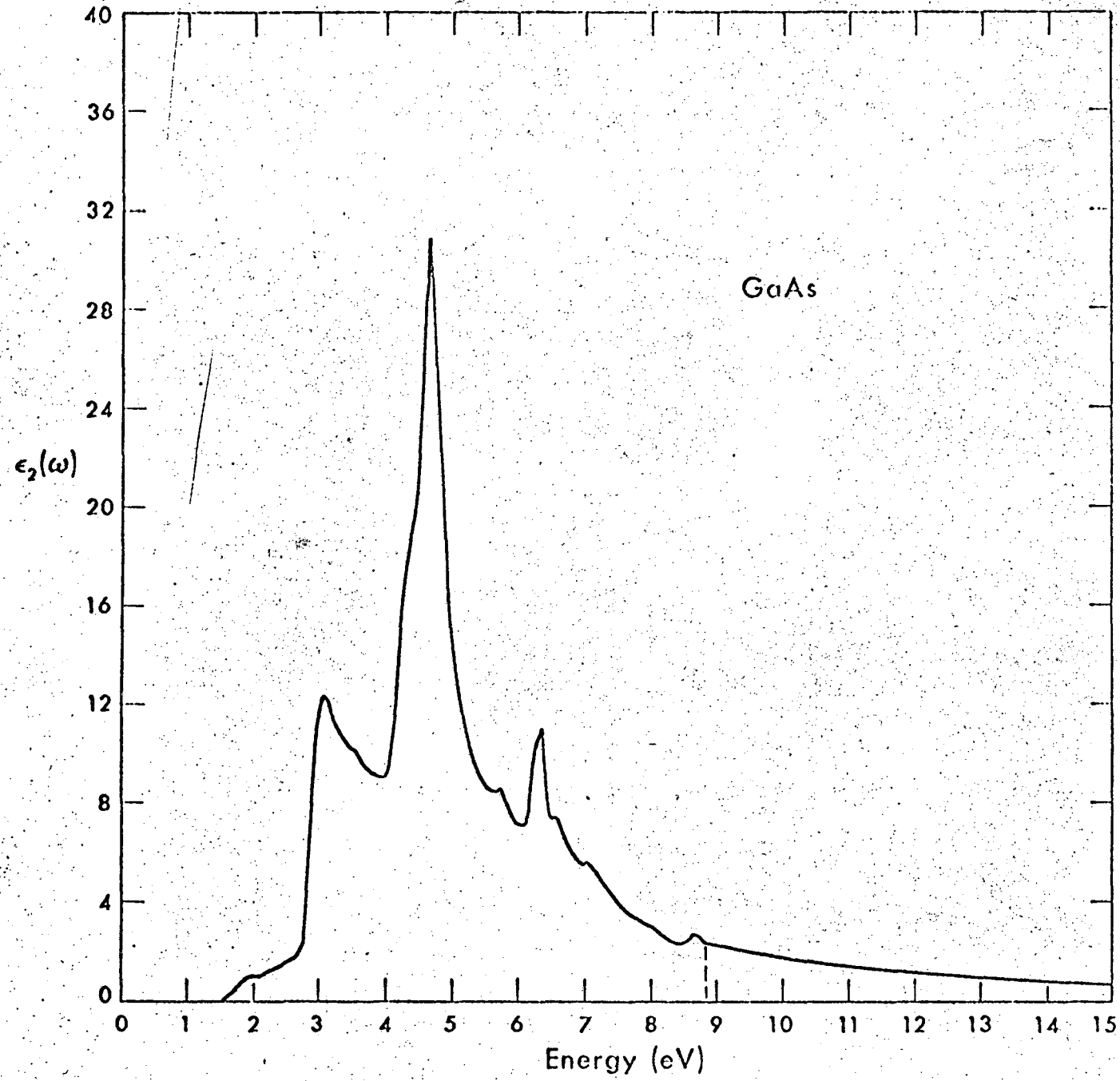
GaAs
$\epsilon_2(\omega)$
Energy (eV)
0
4
8
12
16
20
24
28
32
36
40
0
1
2
3
4
5
6
7
8
9
10
11
12
13
14
15

Fig 2

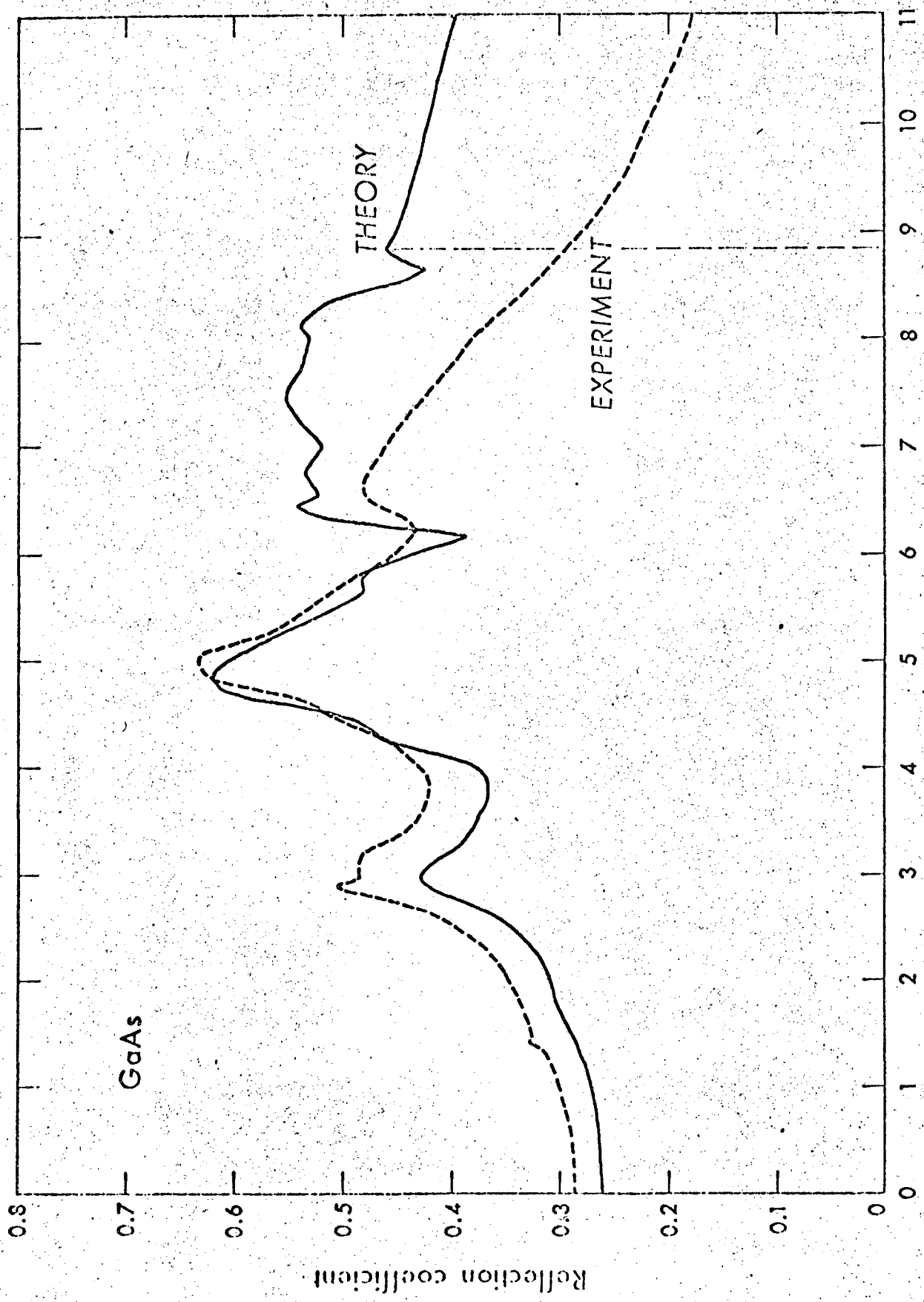
GaAs
THEORY
EXPERIMENT
Reflection coefficient
Energy (eV)
0.8
0.7
0.6
0.5
0.4
0.3
0.2
0.1
0
1
2
3
4
5
6
7
8
9
10
11

Fig. 3

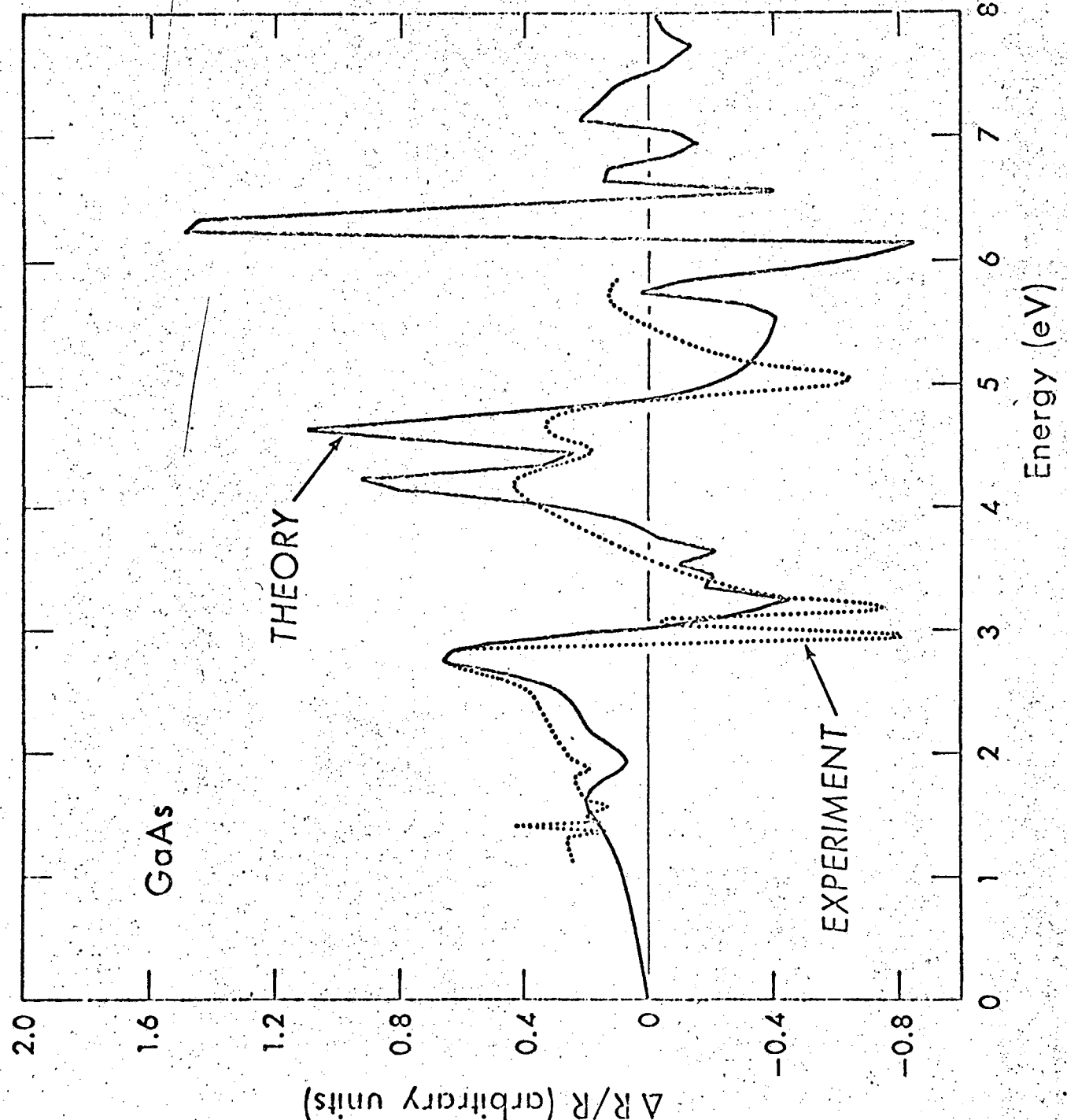
GaAs
THEORY
EXPERIMENT
Energy (eV)
ΔR/R (arbitrary units)
2.0
1.6
1.2
0.8
0.4
0
−0.4
−0.8
0
1
2
3
4
5
6
7
8

Fig. 4

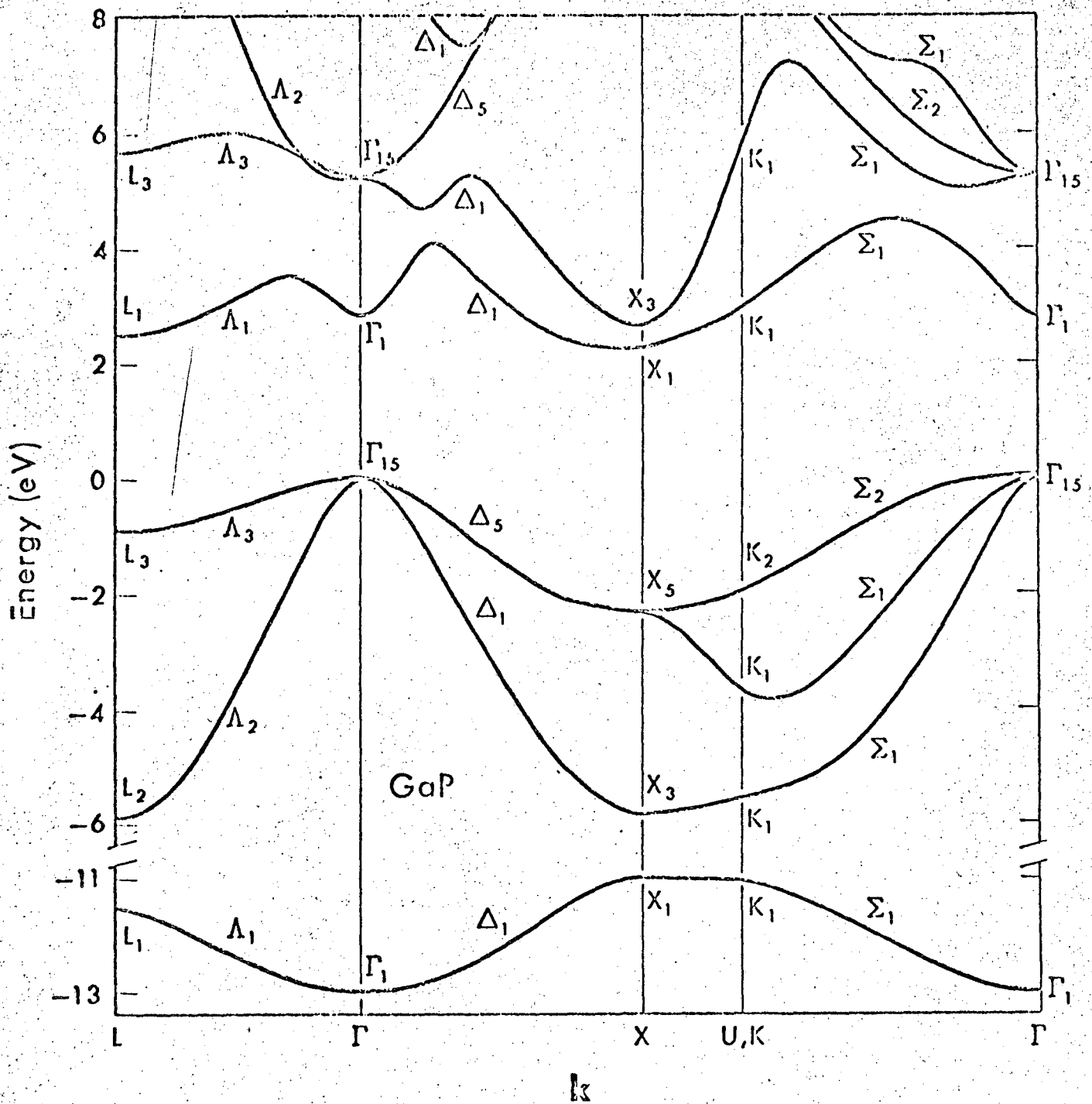
Energy (eV)
8
6
4
2
0
−2
−4
−6
−11
−13
GaP
L
Γ
X
U,K
Γ
k
L3
L1
L2
Λ1
Λ2
Λ3
Γ1
Γ15
Δ1
Δ5
X1
X3
X5
K1
K2
Σ1
Σ2

Fig. 5

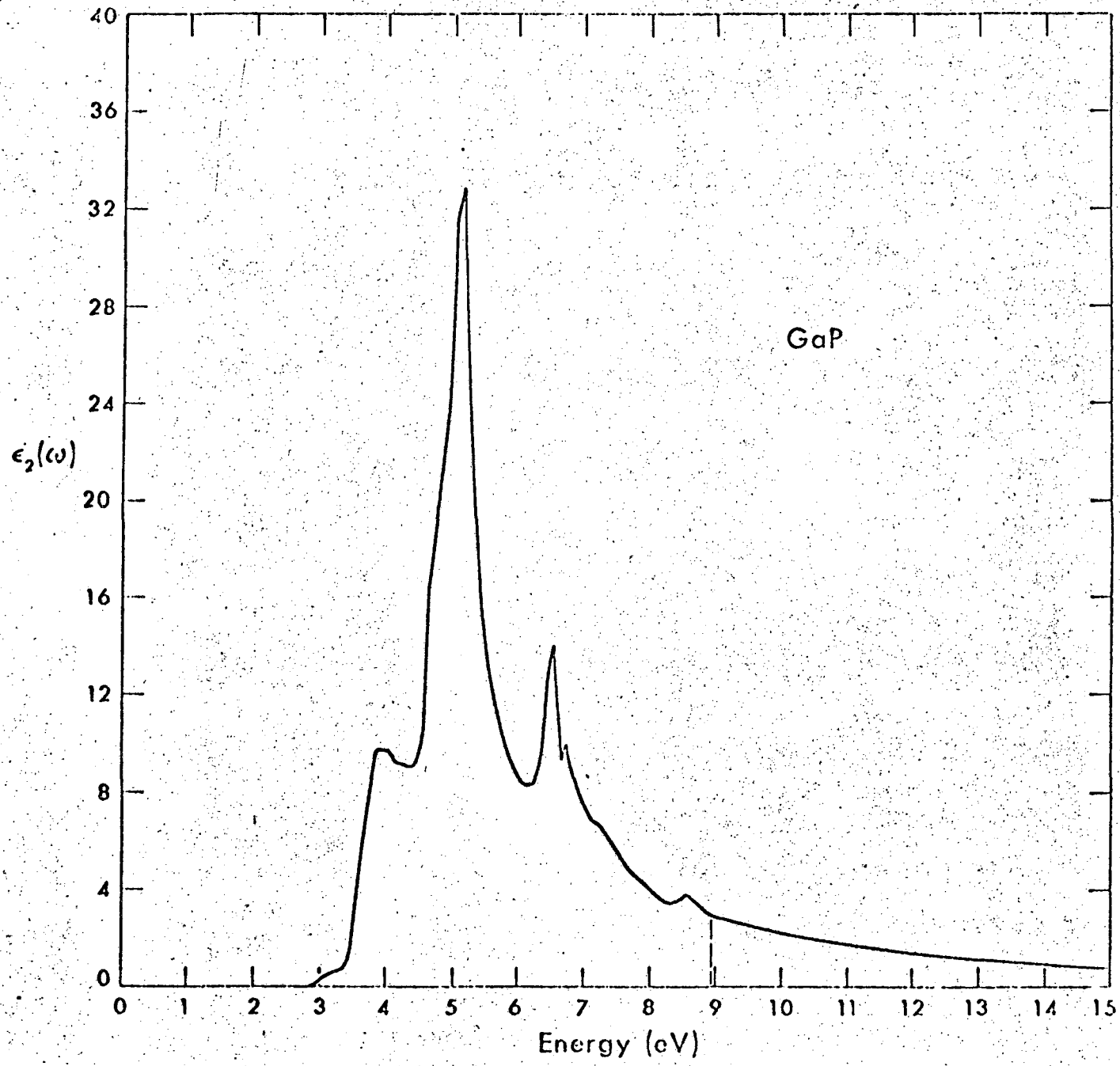
GaP
$\epsilon_2(\omega)$
Energy (eV)
0
4
8
12
16
20
24
28
32
36
40
0
1
2
3
4
5
6
7
8
9
10
11
12
13
14
15

Fig. 6

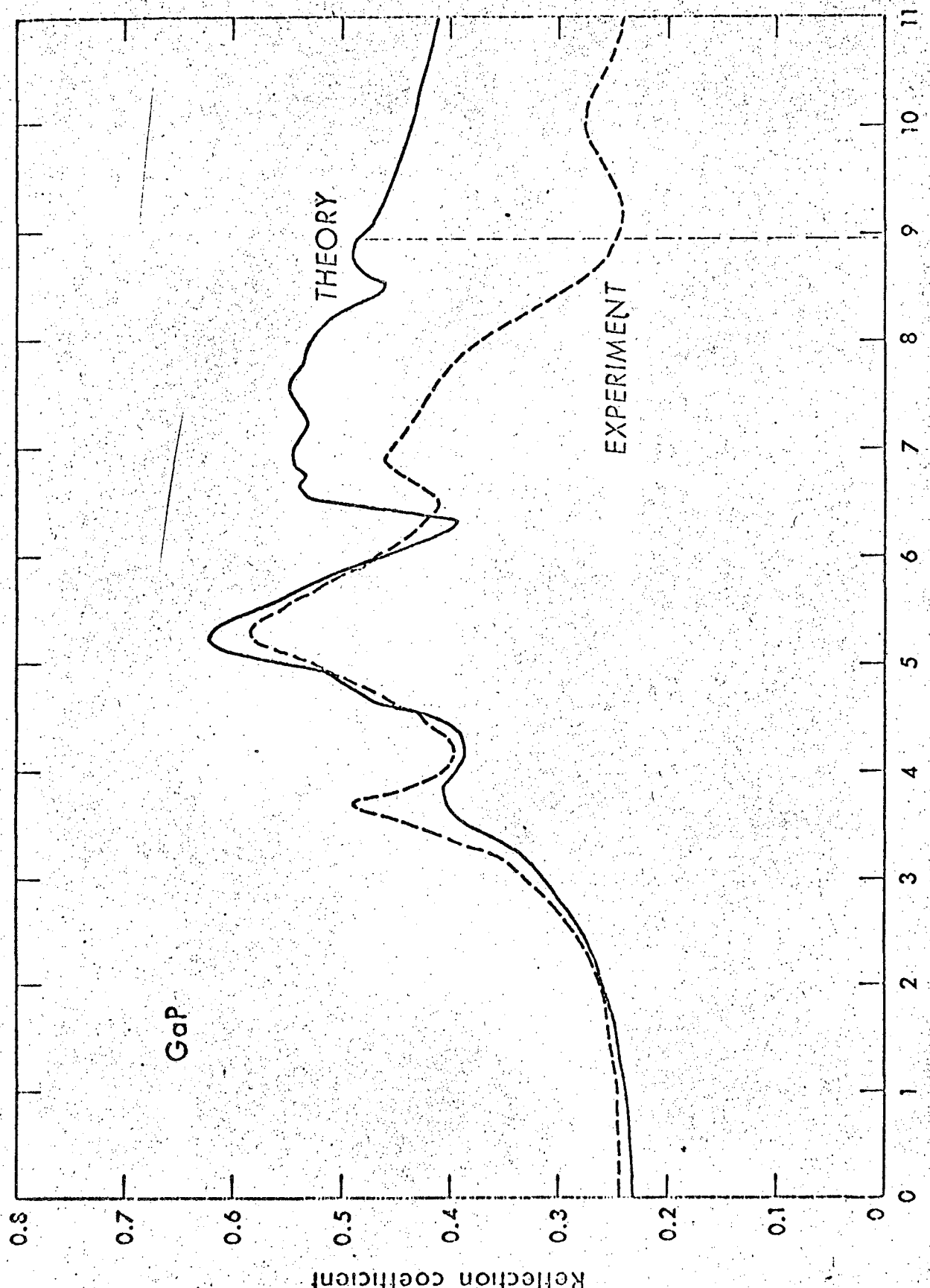
GaP
THEORY
EXPERIMENT
Reflection coefficient
Energy (eV)
0
0.1
0.2
0.3
0.4
0.5
0.6
0.7
0.8
0
1
2
3
4
5
6
7
8
9
10
11

Fig. 7

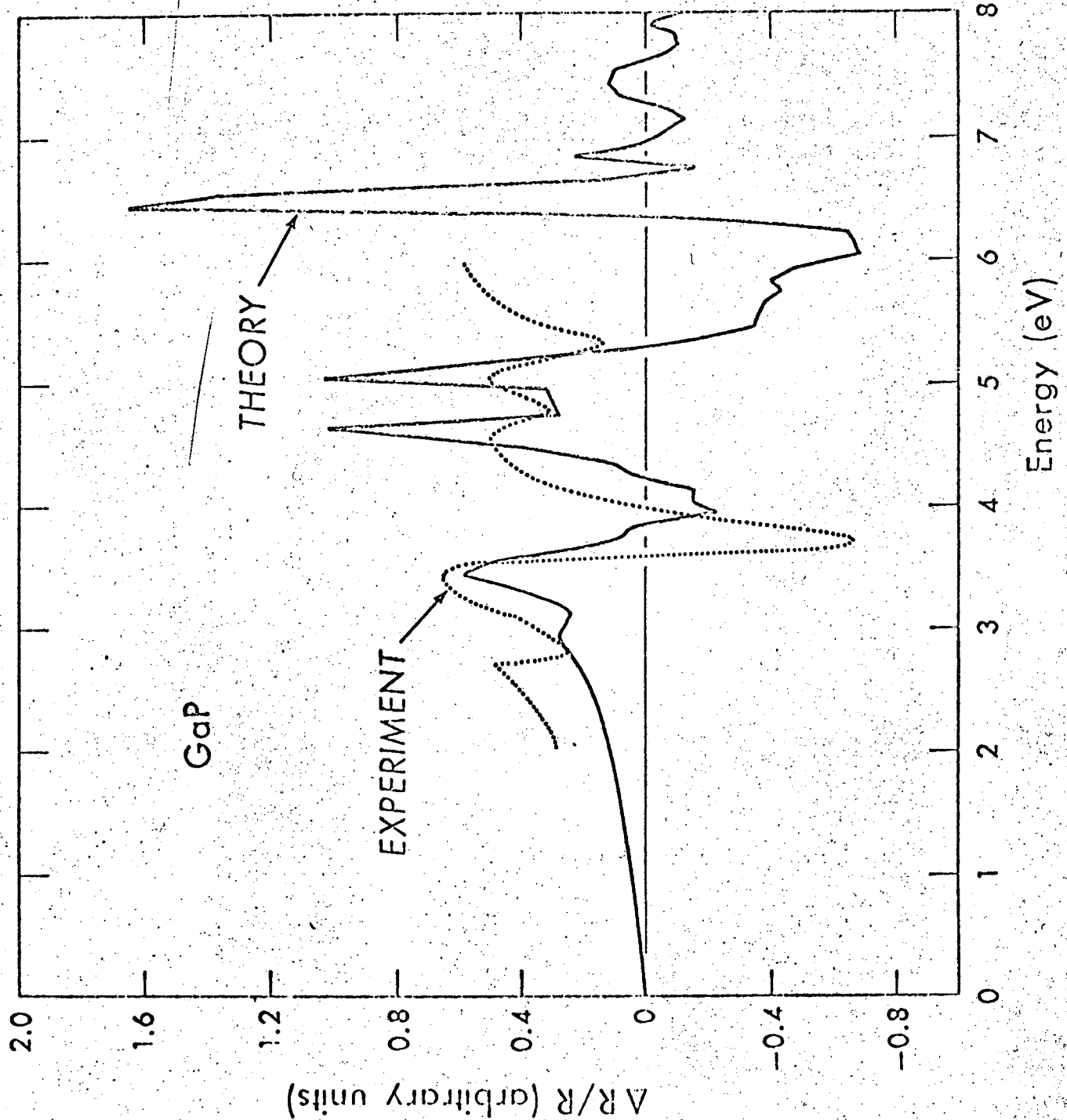
GaP
THEORY
EXPERIMENT
Energy (eV)
ΔR/R (arbitrary units)
2.0
1.6
1.2
0.8
0.4
0
−0.4
−0.8
0
1
2
3
4
5
6
7
8

Fig. 8

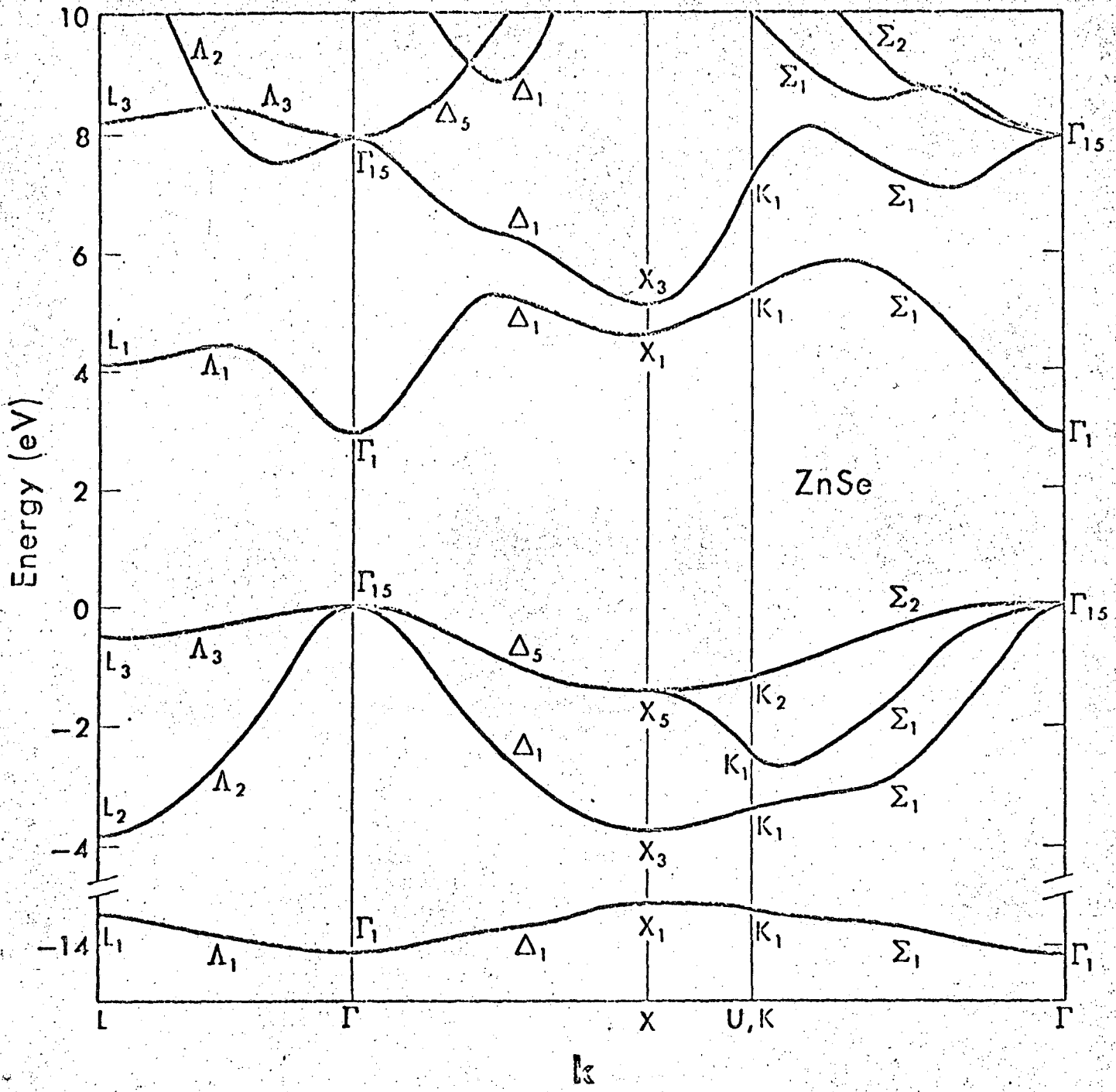
10
8
6
4
2
0
−2
−4
−14
Energy (eV)
ZnSe
L
Γ
X
U, K
Γ
k
L_3
Λ_2
Λ_3
Δ_5
Δ_1
Γ_{15}
Σ_2
Σ_1
K_1
X_3
L_1
Λ_1
Γ_1
X_1
K_2
X_5
L_2

Fig. 9

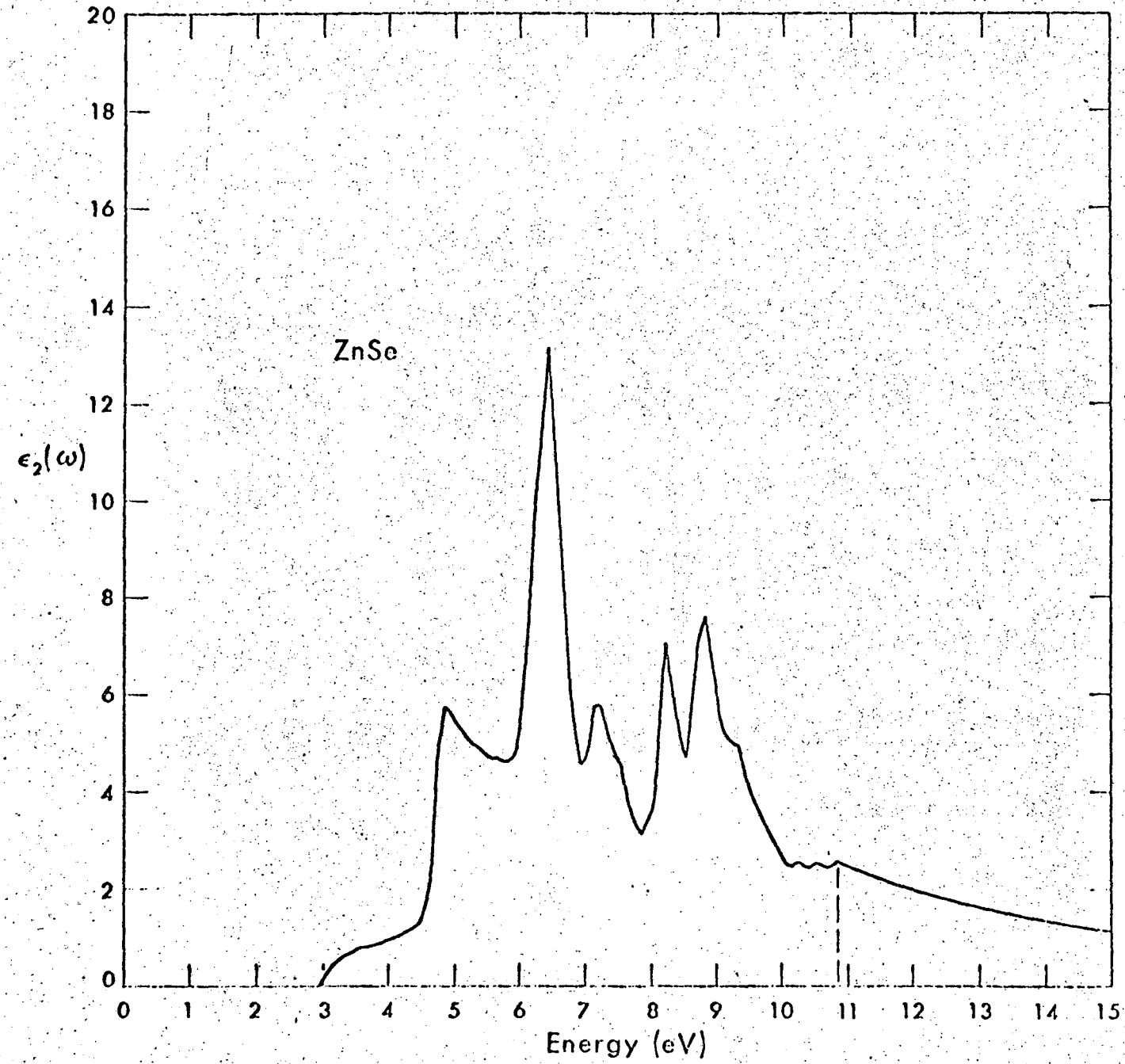
ZnSe
$\epsilon_2(\omega)$
Energy (eV)
0
2
4
6
8
10
12
14
16
18
20
0
1
2
3
4
5
6
7
8
9
10
11
12
13
14
15

Fig. 10

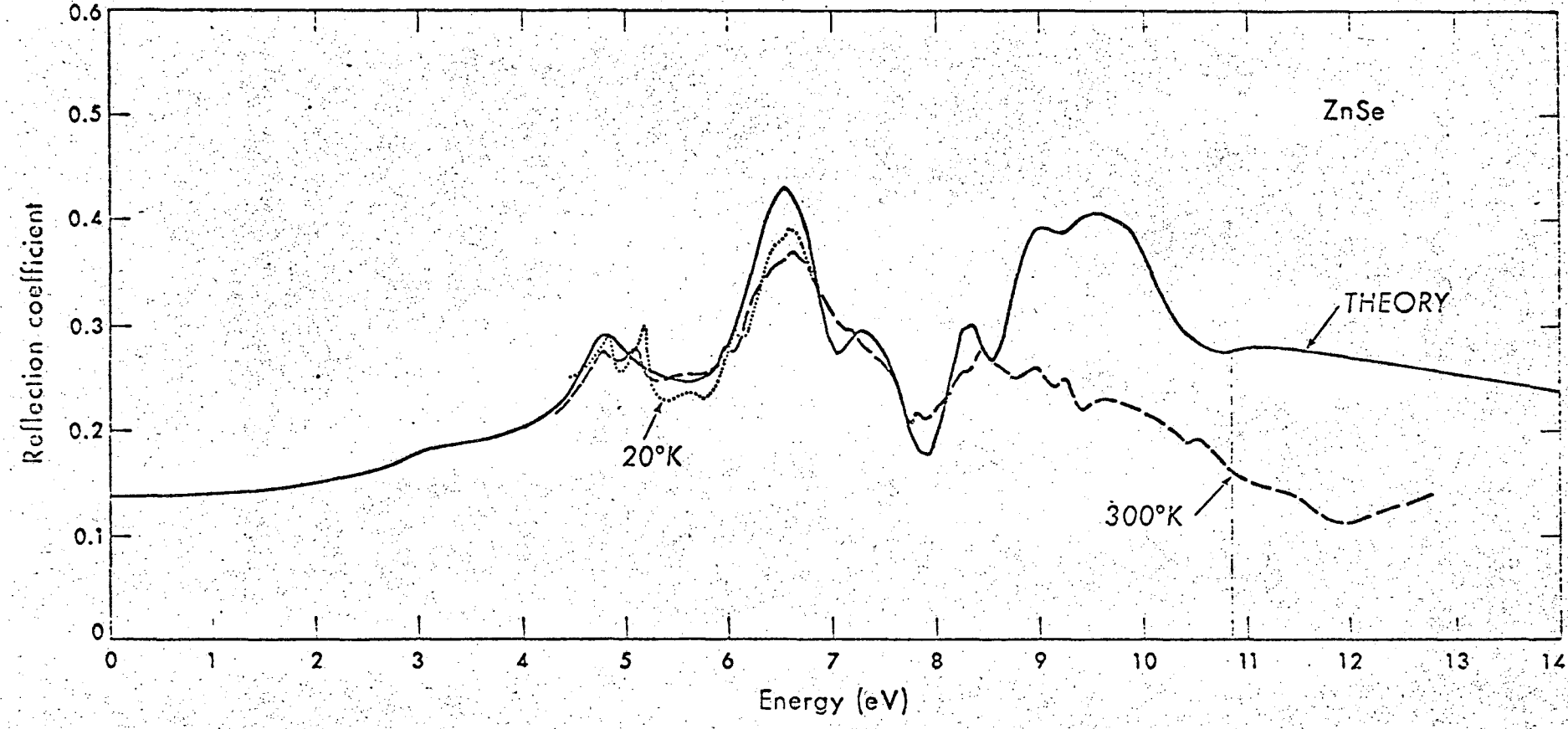
ZnSe
THEORY
20°K
300°K
Reflection coefficient
Energy (eV)
0.6
0.5
0.4
0.3
0.2
0.1
0
0
1
2
3
4
5
6
7
8
9
10
11
12
13
14

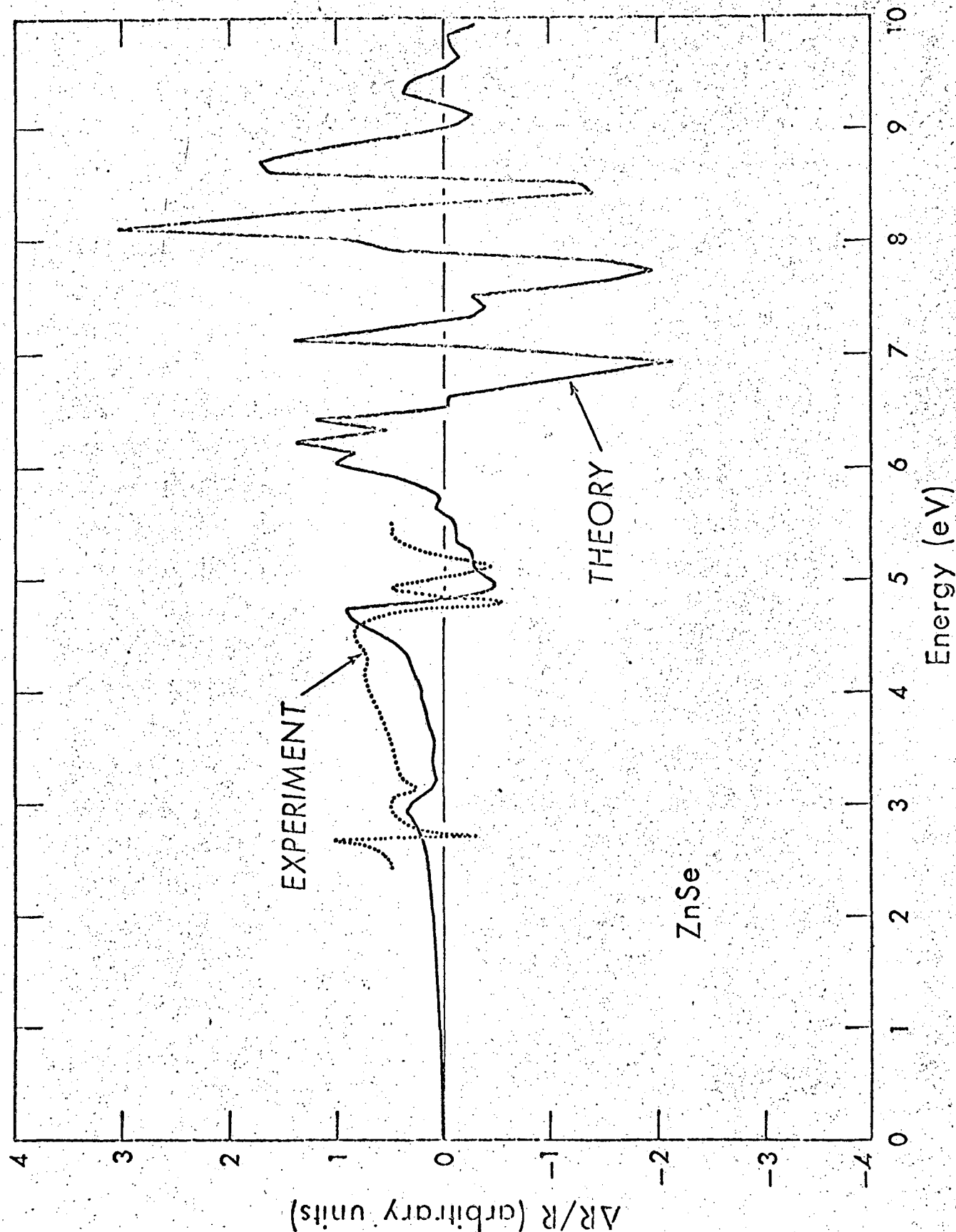
ΔR/R (arbitrary units)
4
3
2
1
0
−1
−2
−3
−4
0
1
2
3
4
5
6
7
8
9
10
Energy (eV)
EXPERIMENT
THEORY
ZnSe

Fig. 12

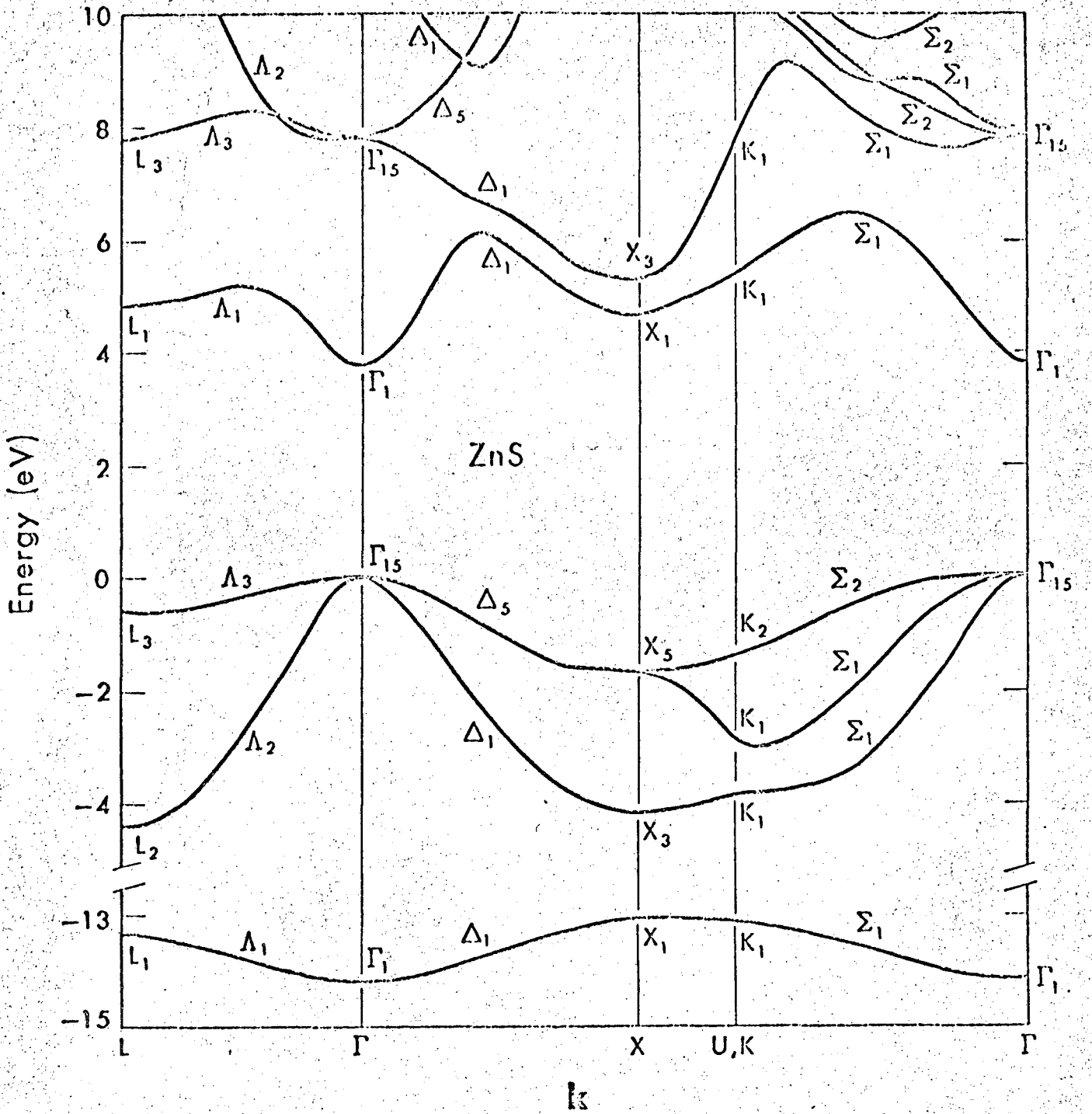
ZnS
Energy (eV)
10
8
6
4
2
0
−2
−4
−13
−15
L
Γ
X
U,K
Γ
k
L3
L1
L2
Λ1
Λ2
Λ3
Δ1
Δ5
Σ1
Σ2
Γ15
Γ1
X1
X3
X5
K1
K2

Fig. 13

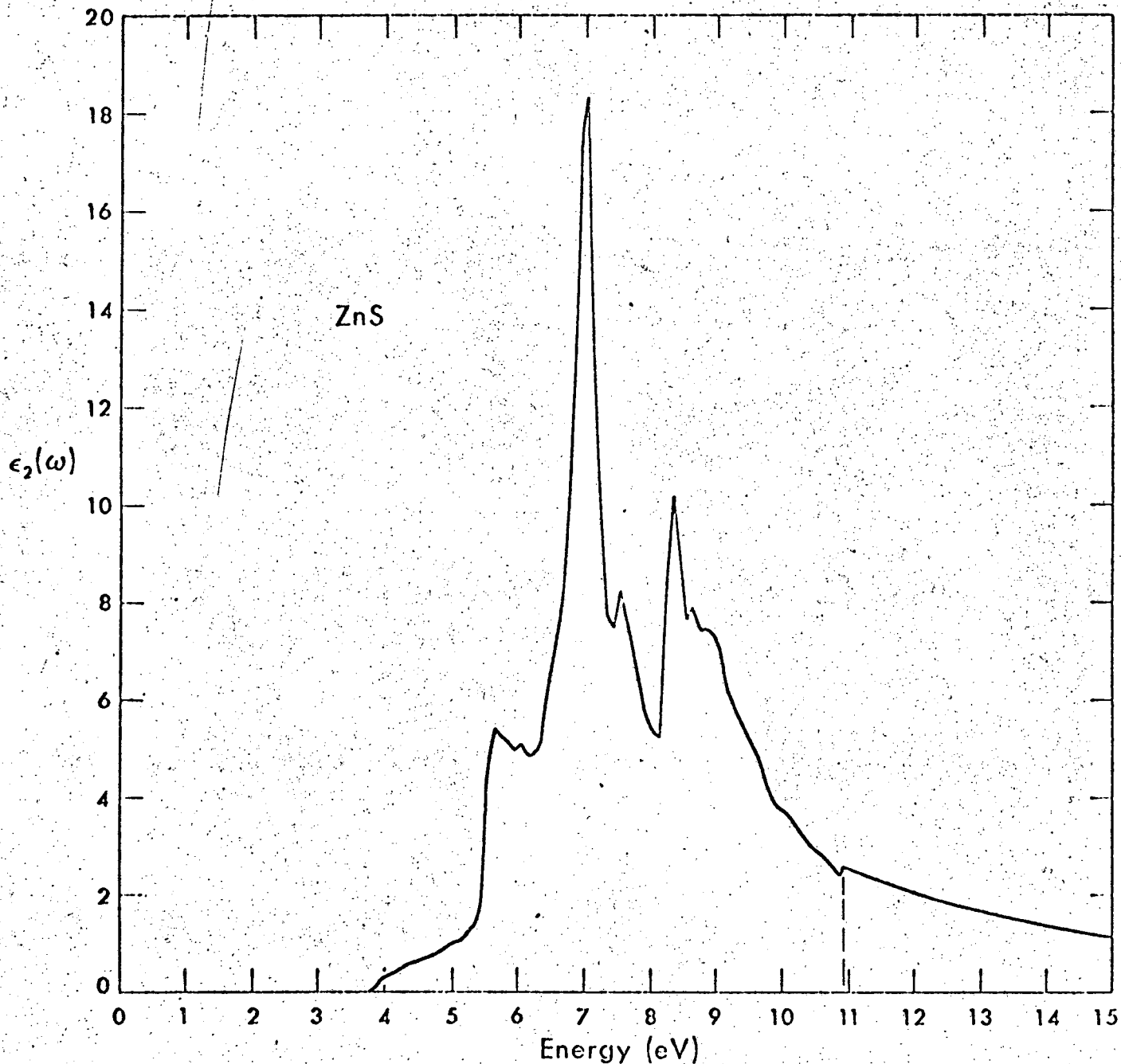
ZnS
$\epsilon_2(\omega)$
Energy (eV)
0
2
4
6
8
10
12
14
16
18
20
0
1
2
3
4
5
6
7
8
9
10
11
12
13
14
15

Fig. 14

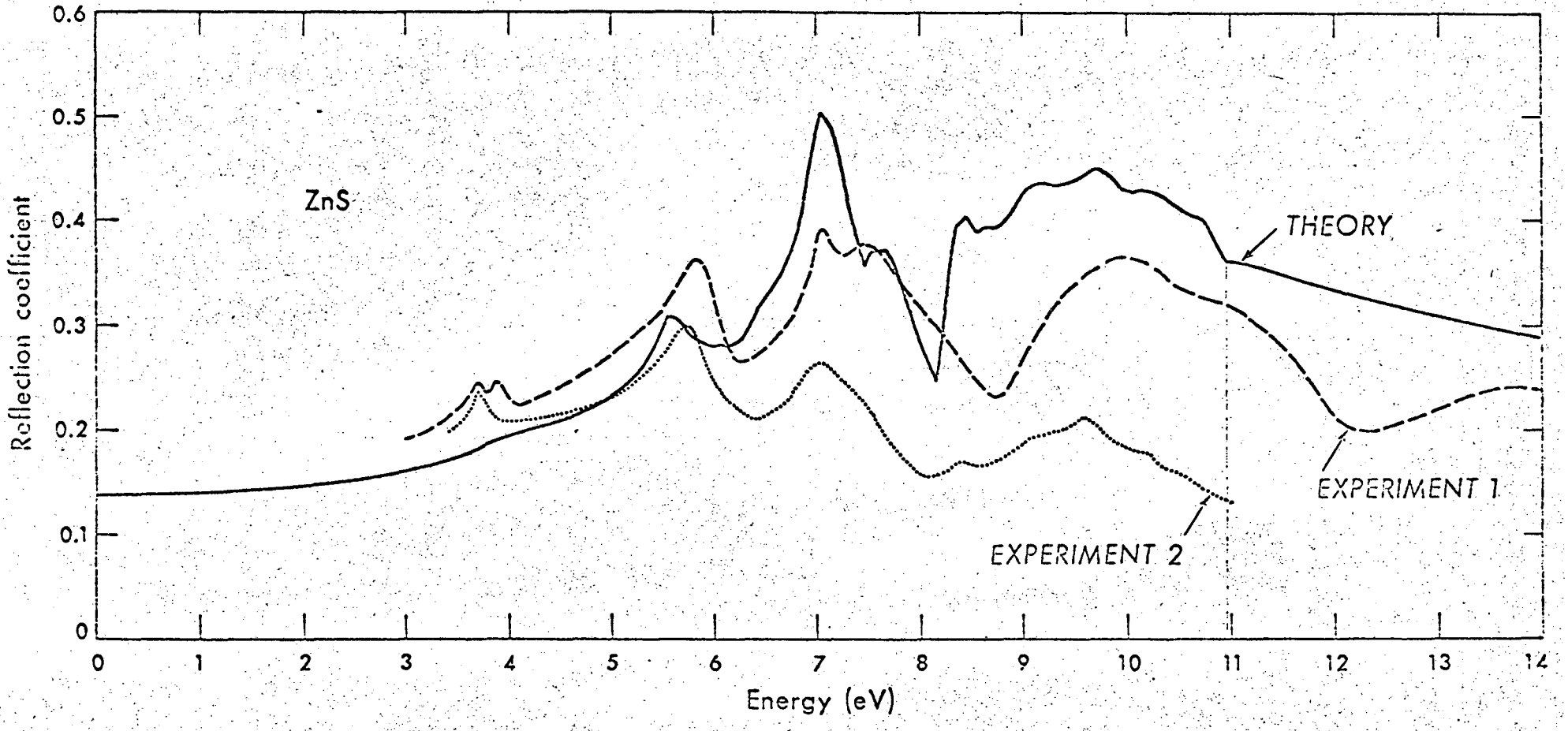
ZnS
THEORY
EXPERIMENT 1
EXPERIMENT 2
Reflection coefficient
Energy (eV)
0.6
0.5
0.4
0.3
0.2
0.1
0
0
1
2
3
4
5
6
7
8
9
10
11
12
13
14

Fig. 15

TECHNICAL INFORMATION DIVISION
LAWRENCE RADIATION LABORATORY
UNIVERSITY OF CALIFORNIA
BERKELEY, CALIFORNIA 94720